

Synthesis and Electrochemical and Biological Studies of Novel Coumarin–Chalcone Hybrid Compounds

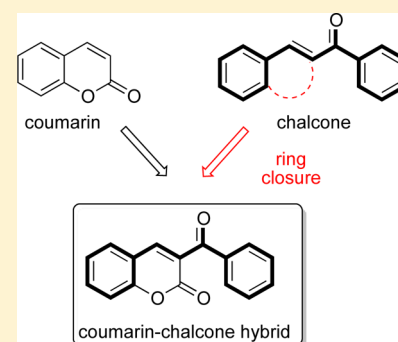
Fernanda Pérez-Cruz,[†] Saleta Vazquez-Rodriguez,^{*,‡} Maria João Matos,[‡] Alejandra Herrera-Morales,[†] Frederick A. Villamena,[§] Amlan Das,[§] Bhavani Gopalakrishnan,[§] Claudio Olea-Azar,^{*,†} Lourdes Santana,[‡] and Eugenio Uriarte[‡]

[†]Free Radical and Antioxidants Laboratory, Inorganic and Analytical Department, Faculty of Chemical and Pharmaceutical Sciences, University of Chile, Sergio Livingstone Polhammer 1007, Independencia, Santiago, Chile

[‡]Department of Organic Chemistry, Faculty of Pharmacy, University of Santiago de Compostela, Campus Vida s/n, 15782, Santiago de Compostela, Spain

[§]Department of Pharmacology and Davis Heart and Lung Research Institute, College of Medicine, The Ohio State University, Columbus, Ohio 43210, United States

ABSTRACT: A series of novel hydroxy-coumarin–chalcone hybrid compounds **2a–i** has been synthesized by employing a simple and efficient methodology. An electrochemical characterization using cyclic voltammetry and ESR spectroscopy were carried out to characterize the oxidation mechanism for the target compounds. The antioxidant capacity and reactivity were determined by ORAC and ESR assays, respectively. Biological assays were assessed to evaluate the cytotoxicity and cytoprotection capacity against ROS/RNS on BAEC. The results revealed that all tested compounds present ORAC values that are much higher than other well-known antioxidant compounds such as quercetin and catechin. Compound **2e** showed the highest ORAC value (14.1) and also presented a low oxidation potential, good scavenging capacity against hydroxyl radicals, low cytotoxicity, and high cytoprotective activity.



INTRODUCTION

Free radicals and reactive oxygen and nitrogen species (ROS and RNS) are atoms, molecules, or ions possessing at least one unpaired electron; therefore, they are highly reactive with a wide range of other different molecules. They are constantly generated and maintained in balance in biological systems through metabolic processes, and they play important roles in a variety of normal biochemical functions such as cell signaling, apoptosis, gene expression, ion transport, and pathological processes.^{1,2}

It is accepted that ROS/RNS play different roles in vivo. Some of these roles are positive and are related to their involvement in energy production, phagocytosis, regulating cell growth, intercellular signaling, and the synthesis of biologically important compounds.³ However, the overproduction of ROS/RNS can have damaging effects on many molecules. ROS/RNS are capable of oxidizing cellular proteins, nucleic acids, and lipids because they are very small and highly reactive. For example, lipid peroxidation is a free-radical-mediated propagation of oxidative damage to polyunsaturated fatty acids involving several types of free radicals, and termination occurs through enzymatic means or by free-radical scavenging by antioxidants.^{4,5} Therefore, the excess of ROS/RNS causes a disturbance in the prooxidant–antioxidant balance in favor of the former, leading to potential damage, which is known as oxidative stress.^{1,6,7} Oxidative stress considerably contributes to

the pathogenesis of inflammatory and cardiovascular diseases, cancer, diabetes, Alzheimer's disease, autism, and aging among others.^{8–13}

The consumption of natural antioxidants, such as flavonoids, supports the endogenous antioxidant defense system. Both dietary and enzymatic antioxidants are components of interrelated systems that interact with each other to control ROS production and thereby ensuring adequate defenses against oxidative stress.^{14,15}

In this sense, many studies concerning the antioxidant capacity of phenolic compounds of different types (e.g., flavonoids, coumarins, and tanins) have been established, and their physicochemical properties have been correlated with their antioxidant properties.¹⁶ In general, free-radical scavenging, redox potential, and the antioxidant activity of these classes of compounds mainly depends on the number and position of hydrogen-donating hydroxyl groups on the aromatic ring of the phenolic molecules, although it is also affected by other factors.¹⁷ Therefore, low oxidation potentials, the number of hydroxyl groups present, and the existence of electron-donating groups and/or the stabilization of a secondary radical via delocalization through conjugated systems play a key role in the antioxidant activity.^{18–21}

Received: April 16, 2013

Published: July 16, 2013

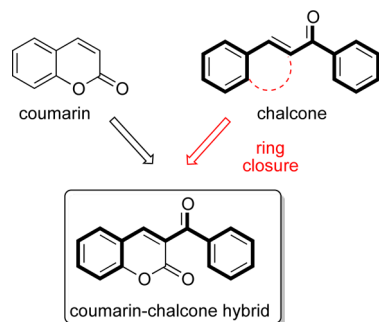
Most of the beneficial health effects of flavonoids are attributed to their antioxidant and chelating abilities. Because of their ability to inhibit low-density lipoprotein (LDL) oxidation, flavonoids have demonstrated unique cardioprotective effects.^{22,23} The protective effects of flavonoids in biological systems are attributed to their capacity for transferring electrons to radicals, chelating metal catalysts,²⁴ activating antioxidant enzymes,²⁵ reducing alpha-tocopherol radicals,²⁶ and inhibiting oxidases.²⁷

Chalcones (α -phenyl- β -benzoyl ethylene) are prominent secondary-metabolite precursors of flavonoids and isoflavonoids in plants. Chemically, they consist of two aromatic rings linked by a three-carbon α,β -unsaturated system and are known to exhibit an impressive array of biological properties.^{28–30} Chalcones have attracted much research attention because of their pharmaceutical potential resulting from their radical-scavenging,^{31,32} antitumor,^{33,34} anti-inflammatory,³⁵ and neuro-protective properties.³⁶ Thus, it is reasonable to explore the radical-scavenging properties of the hydroxyl derivatives of chalcones.

However, coumarins (2*H*-chromen-2-one) are a large family of compounds of both natural and synthetic origin that are important because of the pharmacological activities that these kind of compounds display,³⁷ such as antimicrobial,³⁸ monoamine oxidase (MAO) inhibition,^{39–41} antitumor,⁴² adenosine receptor antagonist,⁴³ and antioxidant¹⁷ among others.

Therefore, coumarin and chalcones represent promising scaffolds in the medicinal chemistry realm. Taking into account the previously mentioned features^{18,19} and with the aim of finding new chemical structures with antioxidant activity, we have designed a new scaffold in which the chalcone fragment is partially incorporated in the coumarin moiety. The resulting coumarin–chalcone hybrid fixes the trans-conformation of the chalcone scaffold by sharing the double bond of the pyrane ring of the coumarin nucleus (Scheme 1).

Scheme 1. Structural Rational Design of Coumarin–Chalcone Hybrid Compounds

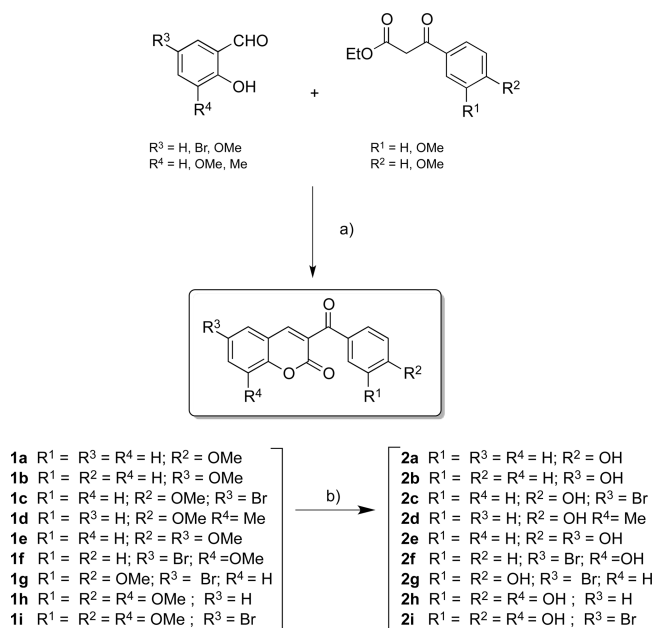


CHEMISTRY

Coumarin derivatives **2a–i** were efficiently synthesized in two steps,⁴⁰ which are briefly described as follows: (i) the synthesis of methoxy-3-benzoylcoumarins **1a–i** and (ii) the synthesis of hydroxy-3-benzoylcoumarins **2a–i**. These steps are outlined in Scheme 2.

On the basis of the widely used Knoevenagel condensation reaction for the preparation of coumarin derivatives,^{37,44} we used an efficient one-step synthesis to generate methoxy-3-benzoylcoumarin precursors **1a–i**. These compounds were prepared in good yields (74–98%) using the appropriately

Scheme 2. Synthesis of Methoxylated (**1a–i**) and Hydroxylated (**2a–i**) 3-Benzoylcoumarin Derivatives^a



^aReagents and conditions: (a) piperidine, EtOH, reflux, 2–5 h; (b) BBr₃, DCM, 80 °C, 48 h.

substituted salicylaldehyde and the corresponding β -keto ester in the presence of piperidine in ethanol under reflux for 2–5 h, obtaining the desired compound as a precipitate that was separated by filtration and further purified by recrystallization in MeOH/DCM. Final compounds **2a–i** were then synthesized by the hydrolysis of the corresponding methoxy precursors **1a–i** by employing an excess of a Lewis acid, BBr₃, in DCM at 80 °C in a Schlenk tube for 48 h followed by treatment with MeOH and purification by flash chromatography of the crude product (69–98%).

ELECTROCHEMICAL STUDY

Cyclic Voltammetry. The electrochemical properties of hydroxy-coumarin–chalcone derivatives **2a–i** were studied by cyclic voltammetry, employing an electrochemical cell with three electrodes and different scan rates between 0.050 and 0.75 V* s⁻¹. Under these conditions, all derivatives exhibited one (compounds **2a–g**) or two (compounds **2h** and **2i**) anodic peaks without the corresponding cathodic peak (Figure 1). The anodic peak potentials (Epa I and Epa II) obtained at a 0.75 V* s⁻¹ scan rate are listed in Table 1.

Characterization of Coumarin–Chalcone Radicals by ESR Spectroscopy. To confirm the formation of semiquinone radicals from compounds **2a–i**, an electron spin resonance (ESR) spectroscopy study was performed. For compounds **2a–d** and **2g**, the spin trap PBN was used. This nitron derivative is a diamagnetic compound that, in the presence of free radicals, produces a spin adduct (paramagnetic species), increasing the half-life of the radicals species.⁴⁵ The experiment was carried out by electrolysis of the derivatives to control the potential in situ using DMSO as the solvent and TBAP as the supporting electrolyte at room temperature. Next, the PBN spin trap was added. In the absence of the PBN spin trap, an ESR spectrum was observed for derivatives **2e**, **2f**, **2h**, and **2i**. Compound **2e**, with two hydroxyl groups, evidenced a symmetric ESR

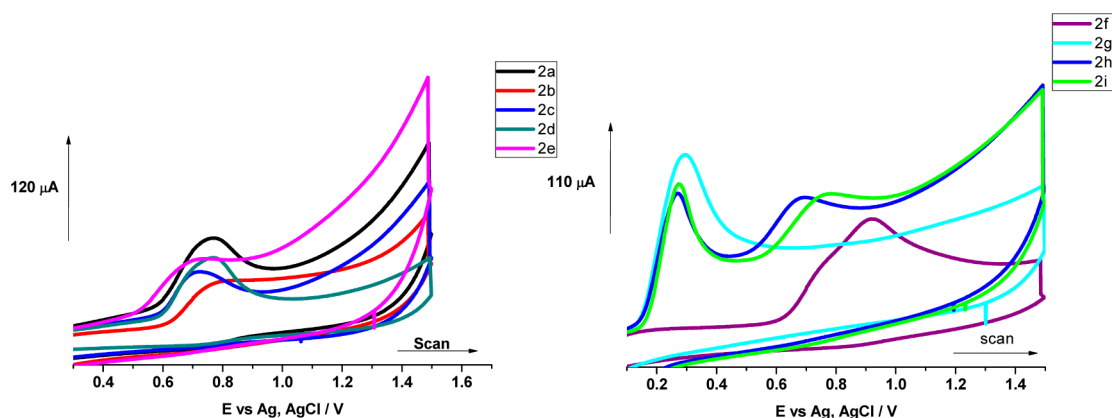


Figure 1. Cyclic voltammograms of the hydroxy-coumarin–chalcone derivatives **2a–i** in phosphate buffer, pH 7.4, at $0.75 \text{ V}^* \text{ s}^{-1}$.

Table 1. Oxidation Potential for Compounds **2a–i^a**

compound	Epa I (V)	Epa II (V)
2a		0.77
2b		0.79
2c		0.72
2d		0.77
2e		0.74
2f		0.92
2g	0.30	
2h	0.27	0.69
2i	0.27	0.77

^aValues obtained at a scan rate of $0.75 \text{ V}^* \text{ s}^{-1}$.

spectrum with five lines (Figure 2a). Compound **2f** showed a hyperfine pattern with two lines (Figure 2b) and was simulated and characterized by two doublets resulting from two nonequivalent hydrogen atoms.

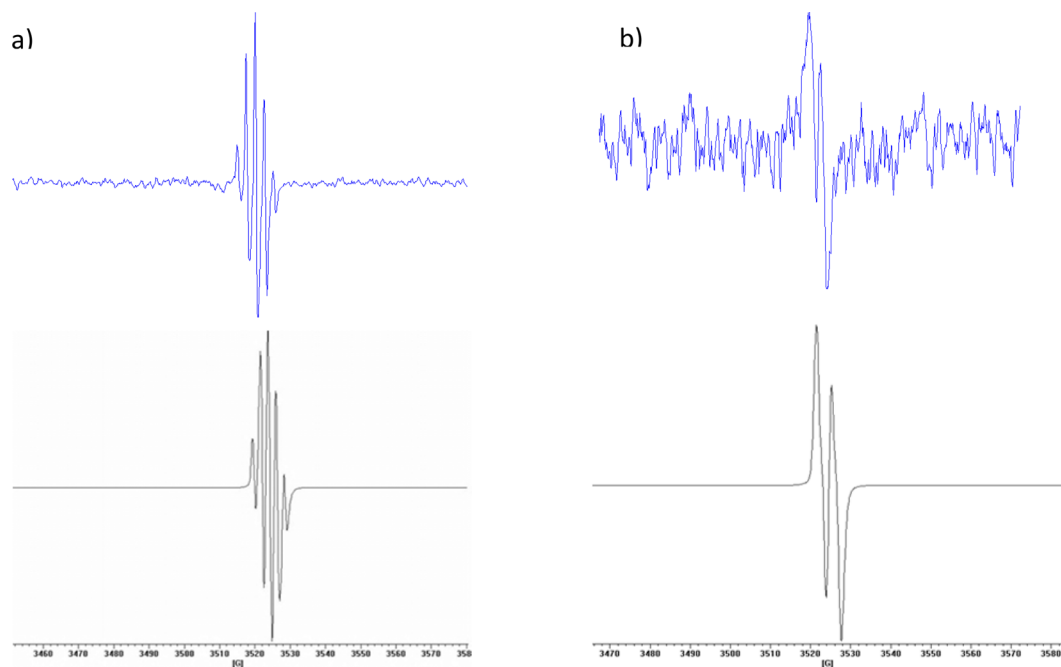


Figure 2. Experimental (blue) and simulated (black) ESR spectra for compounds **2e** (a) and **2f** (b). Simulated hyperfine splitting constants (hfscs) were $a_{\text{H}} = 3.57$ and 1.34 G for compound **2e** and $a_{\text{H}} = 2.35, 2.35$ (two equivalent hydrogen atom), and 1.75 G for compound **2f**.

ORAC-FL Assay. The capacity for peroxy radical scavenging by coumarin–chalcone hybrids was assessed using the oxygen-radical absorbance capacity (ORAC) assay. This methodology gives an index relative to a standard molecule (Trolox), which is a hydrosoluble analog of vitamin E. The ORAC values obtained for all derivatives are shown in Table 2. All derivatives presented an ORAC index higher than well-known antioxidants quercetin and catechin.⁴⁶ Compound **2e** presented the highest ORAC value of the studied series (14.1).

Antioxidant Reactivity by ESR Assay. The reactivity against a mixture of radical species for all of the studied coumarin derivatives was carried out by adapting the $\text{H}_2\text{O}_2/\text{NaOH}/\text{DMSO}/\text{DMPO}$ system⁴⁷ using a noncatalytic and competitive fenton reaction in which the spin trap DMPO and the antioxidant molecule competes for the hydroxyl, superoxide anion, and methyl radicals.

Four wide hyperfine lines were observed in the control measure (labeled as “blank”, indicating the absence of the tested and antioxidant molecules; Figure 3) because of the

Table 2. ORAC Values and the Percentage of Radicals Scavenging for Compounds 2a–i^a

compound	ORAC value	radical scavenging (%)
2a	9.2 ± 0.4	26
2b	11.5 ± 0.4	39
2c	9.5 ± 0.3	28
2d	10.9 ± 0.3	45
2e	14.1 ± 0.3	58
2f	8.3 ± 0.3	65
2g	13.0 ± 0.4	100
2h	8.1 ± 0.6	75
2i	8.8 ± 0.5	100
Trolox	1.0 ± 0.2	31
quercetion	7.3 ± 0.2 ^b	
catechin	6.8 ± 0.2 ^b	

^aMeasured by ESR spin trapping in competition with DMPO. ^bData obtained from ref 46.

mixture of the DMPO–OH, DMPO–CH₃, and DMPO–O₂^{•-} adducts that formed.

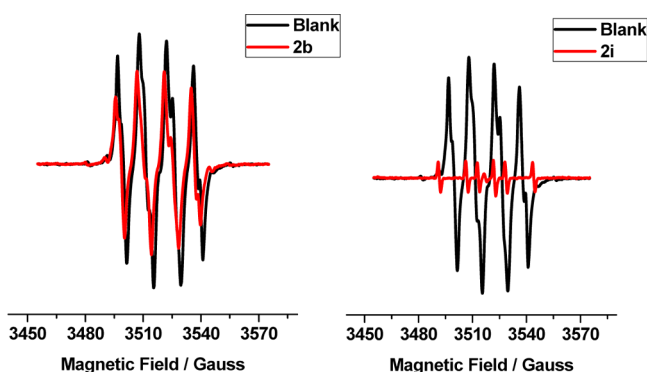


Figure 3. ESR spectra for the reactivity assays of compounds 2b and 2i.

BIOLOGY

Cytotoxicity Assays. The cytotoxicity of compounds 2a–i on bovine aortic endothelial cells (BAEC) was assessed and evaluated over a concentration range of 0–50 μM by employing the 3-(4,5-dimethylthiazol-2-yl)-2,5-diphenyl-2H-tetrazolium bromide (MTT) assay.⁴⁷ The results are shown in Table 3 for concentrations of 10, 20, and 50 μM for each compound studied.

Table 3. Cytotoxicity of Compounds 2a–i tested at Three Different Concentrations on BAEC^a

compound	10 μM	20 μM	50 μM
2a	76 ± 7	60 ± 6	44 ± 5
2b	88 ± 2	95 ± 2	86 ± 1
2c	95 ± 3	93 ± 9	104 ± 6
2d	87 ± 7	82 ± 5	101 ± 8
2e	68 ± 1	94 ± 5	93 ± 10
2f	96 ± 3	101 ± 1	93 ± 4
2g	102 ± 4	100 ± 5	92 ± 5
2h	49 ± 2	68 ± 2	63 ± 2
2i	64 ± 2	23 ± 2	71 ± 6

^aThe results are expressed as the percentage of cell viability (n = 3).

Cytoprotection Assays: ROS/RNS Scavenging Activity in Cell Systems. Hydrogen Peroxide. To evaluate the cytoprotection against H₂O₂, derivatives presenting high cell-viability values (compounds 2b–g) were selected. These compounds also presented high antioxidant capacity in ORAC assays and showed notable hydroxyl-radical scavenging activity.

BAEC were incubated with two different concentrations of each derivative (10 and 20 μM) for 24 h in a 24-well plate followed by treatment with 1 mM H₂O₂ for 2 h. Cell viability was then quantified by the MTT reduction assay (Figure 4a).

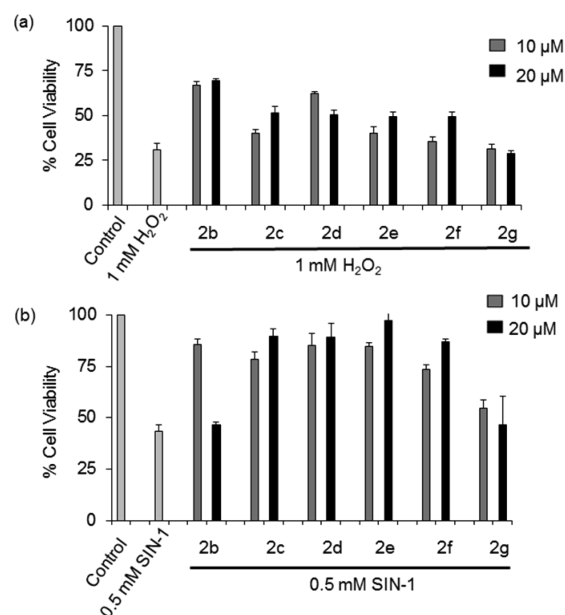


Figure 4. Cytoprotection of compounds 2b–g at 10 and 20 μM against 1 mM H₂O₂- (a) and 0.5 mM SIN-1-induced (b) cytotoxicity of bovine aortic endothelial cells using MTT assay.

Peroxynitrite. The cytoprotective property of the compounds against peroxynitrite in BAEC was investigated by MTT assay. Peroxynitrite was generated in the cells using 3-morpholino-sydnominine (SIN-1).⁴⁸ Figure 4b shows the results for the cytoprotection assays against peroxynitrite for compounds 2b–g.

Theoretical Evaluation of ADME Properties. To correlate better the druglike properties of the coumarin–chalcone hybrid compounds, the lipophilicity, expressed as the octanol/water partition coefficient and herein called log *P*, as well as other theoretical calculations such as the topological polar surface area (TPSA), the number of hydrogen-bond acceptors, and the number of hydrogen-bond donors were calculated using the Molinspiration property program.⁴⁹ The theoretical prediction of the absorption, distribution, metabolism, and excretion (ADME) properties of all compounds is summarized in table 4.

RESULTS AND DISCUSSION

Taking into account the importance of the hydroxyl substituents in the antioxidant properties,^{17,50} we have focused this study on hydroxy-coumarin–chalcone hybrids. All coumarin derivatives described in this Article (compounds 1a–i and 2a–i) were efficiently synthesized according to the simple and generalized experimental procedure outlined in

Table 4. Theoretical Prediction^a of the ADME Properties of Compounds 2a–i

compound	log P	molecular weight	TPSA (Å ²)	n–OH acceptors	n–OHNH donors	volume (Å ³)
2a	2.92	266.25	67.51	4	1	227.00
2b	2.89	266.25	67.51	4	1	227.00
2c	3.70	345.15	67.51	4	1	244.88
2d	3.32	280.28	67.51	4	1	243.56
2e	2.42	282.25	87.74	5	2	235.01
2f	3.89	345.15	67.51	4	1	244.88
2g	3.21	361.15	87.74	5	2	252.90
2h	2.16	298.25	107.97	6	3	243.03
2i	2.92	377.15	107.97	6	3	260.92

^aTPSA, topological polar surface area; n–OH, number of hydrogen acceptors; n–OHNH, number of hydrogen bond donors. The data was determined with the Molinspiration calculation software.

Scheme 2. Electrochemical, biological, and theoretical studies were carried out for final tested compounds 2a–i.

From the experimental results obtained by cyclic voltammetry, we observed that under these conditions all derivatives exhibited one (compounds 2a–g) or two (compounds 2h and 2i) characteristic anodic peaks without the corresponding cathodic peak (Figure 1), indicating an irreversible oxidation process as a result of the oxidation of one hydroxyl group in any of the aromatic rings, forming the semiquinone radical.

The anodic peak potentials (Epa I and Epa II) obtained at a 0.75 V* s⁻¹ scan rate are listed in Table 1. Monohydroxyl derivatives 2a, 2c, and 2d, which contain a hydroxyl substituent at the para position of the benzoyl moiety, presented an anodic peak potential in the same positive potential range (Epa II = 0.77, 0.72, and 0.77 V, respectively). The same positive potential in derivatives 2a and 2d indicates that the methyl substituent at position eight of the coumarin core in 2d is not relevant in the oxidation process. In contrast, the bromine group in derivative 2c seems to provoke a slight decrease in the anodic peak potential (Epa II = 0.72 V). The same effect is observed for compound 2e (Epa II = 0.74 V) that, in addition to the hydroxyl group present in the benzoyl moiety, also bears an additional hydroxyl group in the coumarin core. Compounds 2b and 2f, with a hydroxyl group in the coumarin moiety, presented oxidation potentials that shifted to more positive values (0.79 and 0.92 V, respectively), disfavoring the oxidation process. This effect is more pronounced for compound 2f because of the interaction through intramolecular hydrogen bonding between the OH group in position eight and the oxygen atom of the pyrone ring as well as the electron-withdrawing properties of this pyrone system.⁵¹

Compounds 2g, 2h, and 2i showed a characteristic peak (Epa I) attributed to the catechol moiety. This oxidation occurred at a low potential (0.30, 0.27, and 0.27 V, respectively) because of the electron-donating effect of the hydroxyl group at the 3' position of the benzoyl moiety as well as the favorable quinone formation as the final product in these derivatives. In addition to this low-potential oxidation peak, compounds 2h and 2i showed an additional second peak that was assigned to the hydroxyl group at position eight of the coumarin core.

The data obtained for the characterization of the coumarin–chalcone radicals by ESR spectroscopy showed that in the absence of the spin trap *N-tert-butyl- α -phenylnitron* (PBN), the oxidation of compounds 2a–d and 2g gave no ESR signal. However, in the presence of PBN, a hyperfine pattern with six lines was observed, corresponding to the formation of a carbon-centered semiquinone spin adduct ($a_H \approx 13.5$ and 2.3 G were found for all compounds).⁵² Compound 2e, with two hydroxyl

groups, evidenced a symmetric ESR spectrum with five lines (Figure 2a), and it was interpreted as a semiquinone radical in which the hyperfine pattern corresponds to one triplet assigned to two equivalent hydrogen atoms with $a_H = 2.37$ G and two doublets corresponding to one non equivalent hydrogen atom with hyperfine constants $a_H = 2.35$ and 1.75 G.

Compound 2f showed a hyperfine pattern with two lines (Figure 2b) and was simulated and characterized by two doublets resulting from two nonequivalent hydrogen atoms with $a_H = 1.34$ and 3.57 G. For the radical species of compound 2h, the ESR spectrum (data not shown) was simulated by two doublets attributed to two nonequivalent hydrogen atoms with $a_H = 4.35$ and 2.37 G. Finally, for the radical species of compound 2i, the hyperfine pattern was interpreted and simulated by four doublets resulting from four nonequivalent hydrogen atoms with hyperfine coupling constants $a_H = 2.82$, 2.93, 2.06, and 1.83 G as well as one triplet with $a_H = 3.37$ G resulting from two equivalent hydrogen atoms.

The antioxidant capacity of compounds 2a–i was studied by ORAC-FL assays. From the data obtained, which is summarized in Table 2, we observed that the difference between the ORAC values could be related to the substituents present in these derivatives. Derivatives 2a and 2b, with one hydroxyl group at the para position of the benzoyl moiety and at the six position of the coumarin scaffold, respectively, presented ORAC values of 9.2 and 11.5, respectively. Compounds 2c and 2d, with a hydroxyl group in the same position as in compound 2a but with an additional bromine substituent in position six of the coumarin or a methyl substituent at the position eight, respectively, presented ORAC values of 9.5 and 10.9, respectively. Derivative 2e, which combines the substitution pattern of compounds 2a and 2b, was found to be the compound with the highest ORAC value (14.1).

However, by structurally comparing compounds 2c and 2g, we observed that the only difference is the presence of an additional hydroxyl group at the 3' position of the benzoyl moiety in compound 2g, forming a catechol function. This modification increases the antioxidant capacity in compound 2g (ORAC = 13.0). ORAC values of around 8 were observed for compounds 2f, 2h, and 2i. In addition to the catechol function, compounds 2h and 2i present an additional hydroxyl group at position eight of the coumarin ring compared to structurally related compound 2g. This additional hydroxyl group could form a hydrogen bond with the oxygen atom of the pyrone ring, disfavoring the transfer of the hydrogen atom.

The antioxidant reactivity of compounds 2a–i was studied by an ESR assay. With this method, it was observed that the

intensity of the spectrum decreased in the presence of the tested coumarin–chalcone hybrid compounds that were added to the system (red line, Figure 3). This behavior was observed in all derivatives **2a–i**, and the percent of the radicals (CH_3^\bullet , OH^\bullet , $\text{O}_2^{\bullet-}$) scavenging activity is represented in Table 2. The scavenging values obtained could be related to the number and position of the hydroxyl substituents. Compounds **2g** and **2i** showed a different hyperfine pattern, which was attributed to the formation of carbon-centered spin adducts (Figure 3), demonstrating that the secondary semiquinone radical for each compound was trapped by the DMPO spin trap and the radical scavenging percentages were close to 100.

In general, the MTT assay only provides qualitative trends for the cytotoxicity of the compounds and the cytoprotective properties. The cytotoxicity of compounds **2a–i** on BAEC using different concentrations (10, 20, and 50 μM) is shown in Table 3. Derivatives **2b–g** showed cell viabilities between 86 and 100% up to the maximum concentration of 50 μM . Compounds **2a**, **2h**, and **2i** showed significant toxicity at 50 μM , whereas compound **2a**, which was the most toxic, resulted in only a 44% viability. The varying degrees in the toxicity of the compounds can be accounted for by several factors, such as the differences in their compartmentalization properties, the nature and concentration of ROS produced, and their ability to scavenge radicals and/or initiate pro-apoptotic signaling pathways.

Because compounds **2a**, **2i**, and **2h** demonstrated significant toxicity, they were not used for the cytoprotection assays. However, compounds **2b–g**, because of their low toxicity, were examined at lower doses of 10 and 20 μM to test their cytoprotection against hydrogen peroxide (H_2O_2) or peroxynitrite (ONOO^-) generated from SIN-1, and the data are shown in Figure 4 panels a and b, respectively. Compounds **2b** and **2d** showed the highest cytoprotection against H_2O_2 compared to all compounds, which presented around 40% cytoprotection at 10 μM . At 20 μM , compounds **2c–2f** were cytoprotective against ONOO^- by ~90–95%, whereas compound **2b** imparted no protection at this concentration. Compound **2g** was not cytoprotective against both H_2O_2 and ONOO^- at any of the concentrations tested. All of the studied compounds showed observable cytoprotection, with remarkable results for compounds **2b–f**. In our previous work,⁵³ it was shown that a lipophilic spin trap such as PBN protects BAEC from H_2O_2 -induced toxicity, whereas more polar DMPO protects the cells more efficiently from ONOO^- . The studied compounds show a better cytoprotective effect against ONOO^- . However, because of the complexity of the mechanisms that are directly and indirectly involved in this assay, it is difficult to determine if a correlation exists between the cytoprotection and partition coefficients because these latter values were theoretically calculated. Moreover, the oxidation potentials may not show a direct correlation with the cytotoxicity/cytoprotection data because of other cellular events that are involved such as variations in the ability of the compounds to redox cycle, subcellular compartmentalization, degradation by cellular oxido-reductants, and the ability to induce (or suppress) nonradical-mediated pro-apoptotic pathways. Therefore, although we would like to determine if a direct correlation exists between the cytotoxicity and physical data, such as the partition coefficient and redox potentials, the complexity of the mechanisms involved in cell viability makes this correlation difficult to realize.^{19,54,55}

From the data obtained for the theoretical evaluation of the ADME properties, one can notice that hybrid compounds **2a–i** do not break any point of the Lipinski's rule of five, making them promising leads for drug candidates.⁵⁶ TPSA and log *P* values are compatible with those described as a predictive indicator of a drug's capacity for membrane penetration.⁵⁷

CONCLUSIONS

In this Article, we describe the synthesis of coumarin–chalcone hybrid compounds by employing the Knoevenagel reaction as a key step for the efficient preparation of a selected series. The electrochemical properties of the studied compounds proved to be excellent, presenting low oxidation potentials, very high ORAC values (all of them were higher than the reference compounds quercetin and catechin), and a high percentage of radical scavenging. In most cases, the compounds presented low cytotoxicity for BAEC in culture even at the highest concentration tested as well as good cytoprotective effects against H_2O_2 and ONOO^- induced cell death. In addition, the whole series of compounds presented good theoretical ADME properties. Therefore, on the basis of these results, the synthesized coumarin–chalcone hybrid compounds can be considered to be promising scaffolds in the studied area.

It is worth noting that compound **2e** presented the highest ORAC value (14.1), good scavenging capacity, low cytotoxicity, and high cytoprotection values, especially against ONOO^- induced cell death (almost 100% cell viability at 20 μM); therefore, it can be considered to be potential candidate as a lead compound for more thorough studies of its antioxidant properties.

EXPERIMENTAL SECTION

Chemistry. Melting points were determined using a Reichert Kofler thermopan or in capillary tubes on a Büchi 510 apparatus and are uncorrected. ^1H and ^{13}C NMR spectra were recorded with a Bruker AMX spectrometer at 300 and 75.47 MHz, respectively, using TMS as the internal standard (chemical shifts are given in δ values, *J* is given in Hz). Mass spectra were obtained using a Hewlett-Packard 5988A spectrometer. Elemental analyses were performed using a PerkinElmer 240B microanalyser and were within $\pm 0.4\%$ of calculated values in all cases. Silica gel (Merck 60, 230–00 mesh) was used for flash chromatography (FC). Analytical thin layer chromatography (TLC) was performed on plates precoated with silica gel (Merck 60 F254, 0.25 mm). The purity of compounds **1a–i** and **2a–i** was assessed by HPLC and was found to be higher than 95%. All of the chemical reagents employed in the synthesis process were obtained from Aldrich Chemical Co., Fluka, Across, or Merck (analytical reagent grade). All reactions were carried out under a deoxygenated and dry argon atmosphere unless otherwise indicated. Argon was dried by flowing it through CaCl_2 columns, NaOH stones, and P_2O_5 .

General Procedure for the Synthesis of Methoxy-3-benzoylcoumarins 1a–i.⁴⁰ To a solution of the appropriate β -ketoester (1 mmol) and the corresponding salicylaldehyde (1 mmol) in ethanol (3 mL) was added piperidine in a catalytic amount. The mixture was refluxed for 2–5 h. After completion (indicated by TLC), the reaction was cooled, and the precipitated was filtered and washed with cold ethanol and ether to afford the desired compound. The compounds were further recrystallized from $\text{MeOH}/\text{CH}_2\text{Cl}_2$.

6-Bromo-3-(4'-methoxybenzoyl)coumarin (1c). Yellow solid. Yield: 92%. mp 222–224 °C. ^1H NMR (300 MHz, $\text{DMSO}-d_6$) δ 8.25 (s, 1H, H-4), 8.05 (s, 1H, H-5), 7.92 (d, *J* = 8.5 Hz, 2H, H-2', H-6'), 7.84 (d, *J* = 8.7 Hz, 1H, H-7), 7.44 (d, *J* = 8.7 Hz, 1H, H-8), 7.05 (d, *J* = 8.5 Hz, 2H, H-3', H-5'), 3.85 (s, 3H, OCH_3). ^{13}C NMR (75 MHz, $\text{DMSO}-d_6$) δ 190.1, 164.5, 158.1, 153.5, 143.3, 135.9, 132.7, 131.9, 129.0, 128.3, 120.6, 119.0, 116.7, 114.6, 56.2. MS (EI) *m/z* (9%):

359/361 (M^+ , 28), 135 (100), 92 (19), 77 (20). Anal. Calcd for $C_{17}H_{11}BrO_4$: C, 56.85; H, 3.09. Found: C, 56.82; H, 3.07.

8-Methyl-3-(4'-methoxybenzoyl)coumarin (1d). White solid. Yield 93%. mp 250–252 °C. 1H NMR (300 MHz, DMSO- d_6) δ 8.34 (s, 1H, H-4), 7.91 (d, J = 8.7 Hz, 2H, H-2', H-4'), 7.73–7.24 (m, 3H, H-5, H-6, H-7), 7.06 (d, J = 8.7 Hz, 2H, H-3', H-5'), 3.86 (s, 3H, OCH₃), 2.41 (s, 3H, CH₃). ^{13}C NMR (75 MHz, DMSO- d_6) δ 190.2, 164.4, 158.4, 152.9, 152.8, 144.7, 134.7, 132.3, 129.6, 127.7, 125.8, 124.7, 118.5, 114.6, 56.1, 15.0. MS (EI) m/z (%): 295 ($[M + 1]^+$, 19), 294 (M^+ , 100), 135 (88), 77 (31). Anal. Calcd for $C_{18}H_{14}O_4$: C, 73.46; H, 4.79; Found: C, 73.39; H, 4.57.

6-Methoxy-3-(4'-methoxybenzoyl)coumarin (1e). Yellow solid. Yield 80%. mp 182–184 °C. 1H NMR (300 MHz, DMSO- d_6) δ 7.84 (s, 1H, H-4), 7.71 (d, J = 8.9 Hz, 2H, H-2', H-6'), 7.13–6.94 (m, 3H, H-5, H-7, H-8), 6.77 (d, J = 8.9 Hz, 2H, H-3', H-5'), 3.83 (s, 3H, OCH₃), 3.71 (s, 3H, OCH₃). ^{13}C NMR (75 MHz, DMSO- d_6) δ 190.2, 164.0, 158.3, 155.9, 148.6, 144.2, 132.3, 128.9, 127.3, 121.1, 118.9, 117.6, 114.2, 111.6, 55.9, 55.8. MS (EI) m/z (%): 311 ($[M + 1]^+$, 29), 310 (M^+ , 92), 135 (100), 92 (22), 77 (27). Anal. Calcd for $C_{18}H_{14}O_5$: C, 69.67; H, 4.55. Found: C, 69.45; H, 4.33.

6-Bromo-3-(3',4'-dimethoxybenzoyl)coumarin (1g). Yellow solid. Yield 98%. mp 223–224 °C. 1H NMR (300 MHz, DMSO- d_6) δ 8.23 (s, 1H, H-4), 8.05 (d, J = 2.4 Hz, 1H, H-5), 7.84 (dd, J = 8.8, 2.4 Hz, 1H, H-7), 7.56 (dd, J = 8.4, 2.0 Hz, 1H, H-6'), 7.52–7.38 (m, 2H, H-8, H-2'), 7.05 (d, J = 8.4 Hz, 1H, H-5'), 3.86 (s, 3H, 4'-OCH₃), 3.81 (s, 3H, 3'-OCH₃). ^{13}C NMR (75 MHz, DMSO- d_6) δ 189.8, 157.7, 154.3, 153.2, 149.0, 142.8, 135.6, 131.6, 128.7, 127.9, 125.8, 120.4, 118.8, 116.4, 111.3, 111.1, 56.1, 55.9. MS (EI) m/z (%): 389/391 (M^+ , 59), 165 (100), 71 (31). Anal. Calcd for $C_{18}H_{13}BrO_5$: C, 55.55; H, 3.37. Found: C, 55.54; H, 3.39.

8-Methoxy-3-(3',4'-dimethoxybenzoyl)coumarin (1h). Pale-yellow solid. Yield: 95%. mp 238–240 °C. 1H NMR (300 MHz, DMSO- d_6) δ 8.28 (s, 1H, H-4), 7.54 (dd, J = 8.2, 2.1 Hz, 1H, H-6'), 7.46 (d, J = 2.1 Hz, 1H, H-2'), 7.43–7.27 (m, 3H, H-5, H-6, H-7), 7.04 (d, J = 8.2 Hz, 1H, H-5'), 3.93 (s, 3H, OCH₃), 3.85 (s, 3H, OCH₃), 3.81 (s, 3H, OCH₃). ^{13}C NMR (75 MHz, DMSO- d_6) δ 190.2, 157.9, 154.1, 148.9, 146.6, 144.6, 143.5, 128.8, 127.1, 125.7, 124.9, 120.7, 119.0, 115.5, 111.1, 111.0, 56.3, 56.0, 55.8. MS (EI) m/z (%): 341 ($[M + 1]^+$, 25), 340 (M^+ , 97), 165 (100), 137 (9), 77 (10). Anal. Calcd for $C_{19}H_{16}O_6$: C, 67.05; H, 4.74. Found: C, 67.06; H, 4.74.

6-Bromo-8-methoxy-3-(3',4'-dimethoxybenzoyl)coumarin (1i). Pale-yellow solid. Yield 90%. mp 276–277 °C. 1H NMR (300 MHz, DMSO- d_6) δ 8.21 (s, 1H, H-4), 7.67–7.49 (m, 3H, H-5, H-7, H-6'), 7.46 (s, 1H, H-2'), 7.04 (d, J = 8.5 Hz, 1H, H-5'), 3.96 (s, 3H, 4'-OCH₃), 3.85 (s, 3H, 8-OCH₃), 3.80 (s, 3H, 3'-OCH₃). ^{13}C NMR (75 MHz, DMSO- d_6) δ 195.3, 155.1, 149.9, 149.8, 148.2, 143.6, 138.1, 129.4, 128.9, 128.7, 126.0, 123.4, 119.0, 116.8, 112.6, 112.0, 59.0, 57.6, 56.7. MS (EI) m/z (%): 418/420 (M^+ , 98), 165 (100), 77 (18). Anal. Calcd for $C_{19}H_{15}BrO_6$: C, 54.43; H, 3.61. Found: C, 54.43; H, 3.62.

General Procedure for the Synthesis of Hydroxy-3-benzoylcoumarins (2a–i).⁴⁰ To the corresponding methoxy-3-benzoylcoumarin (1 mmol), BBr_3 in DCM (20 mmol, 1M) was added in a Schlenk tube. The tube was sealed, and the reaction mixture was heated at 80 °C for 48 h. The resulting crude product was treated with MeOH and rotated to dryness. The obtained precipitate was recrystallized from MeOH or purified by flash chromatography using hexane/ethyl acetate mixtures as the eluent to afford the desired hydroxy derivative.

3-(4'-Hydroxybenzoyl)coumarin (2a). White solid. Yield: 78%. mp 242–243 °C (mp lit. 239 °C).⁵⁸ 1H NMR (300 MHz, DMSO- d_6) δ 10.58 (bs, 1H, OH), 8.30 (s, 1H, H-4), 7.89–7.75 (m, 3H, H-5, H-2', H-6'), 7.78–7.64 (m, 1H, H-7), 7.51–7.37 (m, 2H, H-6, H-8), 6.86 (d, J = 8.8, 2H, H-3', H-5'). ^{13}C NMR (75 MHz, DMSO- d_6) δ 190.1, 163.4, 158.5, 154.3, 144.2, 133.6, 132.9, 129.9, 127.8, 127.5, 125.3, 118.7, 116.7, 115.8. MS (EI) m/z (%): 267 ($[M + 1]^+$, 20), 266 (M^+ , 93), 237 (25), 121 (100), 93 (22), 65 (25). Anal. Calcd for $C_{16}H_{10}O_4$: C, 72.18; H, 3.79. Found: C, 71.83; H, 3.53.

6-Bromo-3-(4'-hydroxybenzoyl)coumarin (2c). Pale-yellow solid. Yield: 73%. mp 295–298 °C. 1H NMR (300 MHz, DMSO- d_6) δ 10.61 (bs, 1H, OH), 8.22 (s, 1H, H-4), 8.05 (d, J = 2.4 Hz, 1H, H-5), 7.93–7.73 (m, 3H, H-7, H-2', H-6'), 7.45 (d, J = 8.8 Hz, 1H, H-8), 6.86 (d, J

= 8.7 Hz, 2H, H-3', H-5'). ^{13}C NMR (75 MHz, DMSO- d_6) δ 190.0, 163.6, 158.1, 153.4, 142.8, 136.2, 133.0, 131.8, 128.5, 127.6, 120.7, 119.0, 116.7, 115.9. MS (EI) m/z (%): 343/345 (M^+ , 49), 121 (100). Anal. Calcd for $C_{16}H_9BrO_4$: C, 55.68; H, 2.63. Found: C, 55.30; H, 2.45.

3-(4'-Hydroxybenzoyl)-8-methylcoumarin (2d). White solid. Yield: 56%. mp 252–253 °C. 1H NMR (300 MHz, DMSO- d_6) δ 10.56 (bs, 1H, OH), 8.27 (s, 1H, H-4), 7.80 (d, J = 8.4 Hz, 2H, H-2', H-6'), 7.63 (d, J = 7.5 Hz, 1H, H-5), 7.57 (d, J = 7.5 Hz, 1H, H-7), 7.30 (t, J = 7.5 Hz, 1H, H-6), 6.86 (d, J = 8.4 Hz, 2H, H-3', H-5'), 2.40 (s, 3H, CH₃). ^{13}C NMR (75 MHz, DMSO- d_6) δ 190.2, 163.4, 158.6, 152.6, 144.6, 134.6, 132.9, 127.8, 127.7, 127.2, 125.6, 124.8, 118.5, 115.9, 15.3. MS (EI) m/z (%): 281 ($[M + 1]^+$, 54), 280 (M^+ , 96), 252 (46), 251 (51), 120 (100), 93 (56), 65 (67). Anal. Calcd for $C_{17}H_{12}O_4$: C, 72.85; H, 4.32. Found: C, 72.67; H, 4.12.

6-Hydroxy-3-(4'-hydroxybenzoyl)coumarin (2e). Brown crystals. Yield: 65%. mp 301–303 °C. 1H NMR (300 MHz, DMSO- d_6) δ 10.58 (bs, 1H, 4'-OH), 9.86 (bs, 1H, 8-OH), 8.21 (s, 1H, H-4), 7.79 (d, J = 8.8 Hz, 2H, H-2', H-6'), 7.37–7.24 (m, 1H, H-5), 7.19–7.01 (m, 2H, H-7, H-8), 6.86 (d, J = 8.8 Hz, 2H, H-3', H-5'). ^{13}C NMR (75 MHz, DMSO- d_6) δ 190.3, 163.4, 158.8, 154.4, 147.7, 144.0, 132.9, 127.8, 127.6, 121.6, 119.2, 117.6, 115.9, 113.7. MS (EI) m/z (%): 283 ($[M + 1]^+$, 9), 282 (M^+ , 51), 121 (100), 93 (15), 65 (18). Anal. Calcd for $C_{16}H_{10}O_5$: C, 68.09; H, 3.57. Found: C, 68.23; H, 3.33.

3-Benzoyl-6-bromo-8-hydroxycoumarin (2f). Pale-yellow solid. Yield: 98%. mp 293–295 °C. 1H NMR (300 MHz, DMSO- d_6) δ 10.92 (s, 1H, OH), 8.30 (s, 1H, H-4), 7.93 (dd, J = 8.1, 1.4 Hz, 2H, H-2', H-6'), 7.79–7.63 (m, 1H, H-5), 7.63–7.44 (m, 3H, H-3', H-4', H-5'), 7.34–7.24 (m, 1H, H-8). ^{13}C NMR (75 MHz, DMSO- d_6) δ 191.9, 157.9, 146.3, 144.8, 142.7, 136.3, 134.5, 130.0, 129.2, 127.8, 121.9, 121.8, 120.9, 116.2. MS (EI) m/z (%): 344/346 (M^+ , 46), 105 (100), 77 (59). Anal. Calcd for $C_{16}H_9BrO_5$: C, 53.21; H, 2.51. Found: C, 52.97; H, 2.41.

6-Bromo-3-(3',4'-dihydroxybenzoyl)coumarin (2g). Yellow solid. Yield: 72%. mp 264–266 °C. 1H NMR (300 MHz, DMSO- d_6) δ 10.14 (s, 1H, OH), 9.47 (s, 1H, OH), 8.19 (s, 1H, H-4), 8.05 (d, J = 2.1 Hz, 1H, H-5), 7.84 (dd, J = 8.8, 2.2 Hz, 1H, H-7), 7.45 (d, J = 8.8 Hz, 1H, H-8), 7.39–7.20 (m, 2H, H-2', H-6'), 6.82 (d, J = 8.1 Hz, 1H, H-5'). ^{13}C NMR (75 MHz, DMSO- d_6) δ 189.6, 157.9, 153.3, 152.5, 145.9, 142.3, 135.7, 131.7, 128.4, 127.8, 124.5, 120.5, 119.0, 116.7, 116.3, 115.7. MS (EI) m/z (%): 360/362 (M^+ , 87), 253 (47), 251 (45), 227 (14), 225 (18), 137 (100), 109 (44). Anal. Calcd for $C_{16}H_9BrO_5$: C, 53.21; H, 2.51. Found: C, 53.23; H, 2.52.

8-Hydroxy-3-(3',4'-dihydroxybenzoyl)coumarin (2h). Bright-yellow solid. Yield: 81%. mp 277–279 °C. 1H NMR (300 MHz, DMSO- d_6) δ 10.35 (s, 1H, OH), 10.10 (s, 1H, OH), 9.47 (s, 1H, OH), 8.20 (s, 1H, H-4), 7.36–7.06 (m, 5H, H-5, H-6, H-7, H-2', H-6'), 6.82 (d, J = 8.2 Hz, 1H, H-5'). ^{13}C NMR (75 MHz, DMSO- d_6) δ 190.2, 158.4, 152.3, 145.8, 145.0, 144.2, 142.8, 128.0, 127.4, 125.3, 124.2, 119.7, 119.5, 116.4, 115.7. MS (EI) m/z (%): 299 ($[M + 1]^+$, 8), 298 (M^+ , 41), 155 (16), 137 (100), 91 (31). Anal. Calcd for $C_{16}H_{10}O_6$: C, 64.43; H, 3.38. Found: 64.43; H, 3.39.

6-Bromo-8-hydroxy-3-(3',4'-dihydroxybenzoyl)coumarin (2i). Pale-yellow solid. Yield 69%. mp 300–302 °C. 1H NMR (300 MHz, DMSO- d_6) δ 10.89 (s, 1H, OH), 10.14 (s, 1H, OH), 9.48 (s, 1H, OH), 8.14 (s, 1H, H-4), 7.45 (d, J = 2.2 Hz, 1H, H-5), 7.38–7.12 (m, 3H, H-7, H-2', H-5'), 6.81 (dd, J = 8.1, 3.0 Hz, 1H, H-6'). ^{13}C NMR (75 MHz, DMSO- d_6) δ 189.3, 157.4, 152.0, 145.8, 145.5, 142.3, 141.9, 128.0, 127.4, 124.0, 121.1, 121.0, 120.5, 115.9, 115.8, 115.2. MS (EI) m/z (%): 376/378 (M^+ , 100), 269 (30), 267 (24), 137 (80), 109 (74). Anal. Calcd for $C_{16}H_9BrO_6$: C, 50.95; H, 2.41. Found: C, 50.92; H, 2.43.

Cyclic Voltammetry. Cyclic voltammetry was carried out using a potentiostat/galvanostat VersaSTAT 3 that was provided with the V3-Studio electrochemistry software package in 50 mM sodium phosphate buffer (pH 7.4) at room temperature using a three-electrode cell. A glassy-carbon electrode was used as the working electrode, a platinum wire, the auxiliary electrode, and Ag, AgCl/KCl (ca. 3.5 M), the reference electrode. All coumarin–chalcone hybrids were studied to 1 mM in 20% methanol as final concentration.

Characterization of Coumarin-Chalcone Radicals by ESR Spectroscopy. ESR measurements were carried out on an ESR spectrometer equipped with a high-sensitivity resonator at room temperature. Unless otherwise indicated, the instrument settings used for general spectral acquisition were microwave power, 10 mW, modulation amplitude, 1 G, receiver gain, 1.0×10^4 or 1.0×10^5 , scan time, 21.5 s, time constant, 40.0 s, and sweep width, 120 G. The oxidation process was carried out by using 30% H_2O_2 and NaOH (25 mM) in the presence of chalcone–coumarin hybrids. Scans were integrated using the Bruker WINEPR v.2.11b software. The sample cells used were 50 μL glass capillary tubes. An automatic fitting program carried out the spectrum simulation. The hyperfine splitting constants were estimated to be accurate to within 0.05 G.

Radical-Generating System to Test Coumarin-Chalcone Hybrids. To the corresponding coumarin–chalcone hybrid compound (1.2 mmol) in dimethyl sulfoxide (20 μL), a hydrogen peroxide solution (50 μL , 30%) and a sodium hydroxide solution (50 μL , 25 mM) were added. The total volume of the resulting solution (300 μL) was completed with DMSO to achieve a final 4 mM solution of the tested compounds.

ORAC-FL Assay. The ORAC-FL assays were carried out on a Synergy HT multidetection microplate reader (Bio-Tek Instruments, Inc.) using white polystyrene 96-well plates. Fluorescence was read from the top, with an excitation wavelength of 485/20 nm and an emission filter of 528/20 nm. The plate reader was controlled by Gen 5 software. The oxygen radical absorbance capacity was determined as previously described⁴⁶ with slight modifications. The reaction was carried out in 75 mM sodium phosphate buffer (pH 7.4) at a 200 μL final volume. FL (70 nM, final concentration) and coumarin–chalcone solutions in methanol with a range of concentration between 0.3 to 2 μM and 0.5 to 7 μM for the monohydroxy and dihydroxy derivatives, respectively, were placed in each well of the 96-well plate. This range of concentration was selected empirically to obtain a good separation between the fluorescence curves. This separation was crucial for more accurate data treatment.^{59,60} The mixture was preincubated for 15 min at 37 °C before rapidly adding the AAPH solution (18 mM, final concentration). The microplate was immediately placed in the reader and automatically shaken prior to each reading. The fluorescence was recorded every 1 min for 120 min. A blank with FL and AAPH using methanol instead of the antioxidant solution as well as five calibration solutions using Trolox (0.5 to 2.5 μM) as a standard molecule were also used in each assay. The inhibition capacity was expressed as ORAC values, and it was quantified by employing eq 1. All reaction mixtures were prepared in triplicate, and at least three independent assays were performed for each sample.

$$\text{relative ORAC value} = \frac{[\text{AUC} - \text{AUC}^0]}{[\text{AUC}_{\text{trolox}} - \text{AUC}^0]} \frac{[\text{trolox}]}{[\text{derivative}]} \quad (1)$$

where AUC^0 = area under the curve blank; AUC = area under the curve derivative; $\text{AUC}_{\text{trolox}}$ = area under the curve Trolox (standard); $[\text{trolox}]$ = Trolox concentration, molar; and $[\text{Derivative}]$ = derivative concentration, molar

The AUC was calculated by integrating the decay of the fluorescence where F_0 is the initial fluorescence read at 0 min and F is the fluorescence read at a particular time. The AUC_{NET} corresponding to the sample was calculated by subtracting the AUC corresponding to the blank. Data processing was performed using Origin Pro 8 SR2 (Origin Lab Corporation).

Antioxidant Reactivity by ESR Assay. The reactivity of all coumarin–chalcone hybrids against hydroxyl radicals was assessed using the noncatalytic Fenton method that was previously described.⁵⁶ In a typical experiment, 150 μL of dimethyl sulfoxide was mixed with 50 μL of NaOH (3 mM) followed by the addition of 50 μL of DMPO (30 mM) spin trap and 50 μL of hydrogen peroxide (30%). All derivatives were studied at a 4 mM final concentration and a 300 μL final volume. The mixture was positioned in the ESR cell, and the spectra were recorded after 5 min of the reaction.

Biological Studies. All chemicals and solvents used were of the highest analytical grade. For cell culture, all reagents or materials were

purchased and used without further purification. Bovine aortic endothelial cells were purchased from Cell Systems (Kirkland, WA) and nonessential amino acids and Fetal Bovine Serum (FBS) were purchased from Gibco and Invitrogen, respectively.

Cell Culture. Cells were cultured in 75 cm^2 tissue-culture flasks using Dulbecco's modified Eagle's medium with 1 g/L of D-glucose and 4 mM L-glutamine and supplemented with 10% fetal bovine serum, 2.5 mg/L of endothelial cell growth supplement, and 1% nonessential amino acids in the absence of antibiotics at 37 °C in a humidified atmosphere of 5% CO_2 and 20% O_2 . The medium was changed every 2 to 3 days, and the cells were subcultured once they reached 80–85% confluence.⁵¹

Cytotoxicity and Cytoprotection. Cytotoxicity assays in BAEC cells were performed for all coumarin–chalcone hybrids using the MTT reduction assay. BAEC were seeded in 24-well plates at a density ranging between 10^4 – 10^5 cells/mL per well. After the cells reached 60–70% confluence, they were incubated in the presence of 10 to 50 μM of the corresponding coumarin–chalcone derivatives for 24 h. After incubation, the medium was changed (2 mL) and 45 μL of a solution of MTT (5 mg/mL in DMEM supplemented with 0.5% FBS) was added to each well. The cells were incubated for another 2 h at 37 °C. The medium was then removed, and the wells were rinsed once with PBS. DMSO (0.6 mL) was added to each well at room temperature to solubilize the formazan crystals. The dissolved formazan was then transferred into 96-well culture plates, and the absorbance was measured at 570 nm using a UV–vis spectrophotometer.^{57,58}

The percent of inhibition of cell viability was calculated using eq 2

$$\text{percent inhibition} = (1 - A_t/A_s)100 \quad (2)$$

where A_t and A_s are the absorbance of the sample solution and the solvent alone, respectively.

To assess the cytoprotective properties of the compounds against H_2O_2 and SIN-1, BAEC (10^4 – 10^5 cells/mL) were grown to 60–70% confluence in 24-well plates and each well was incubated with the selected derivative at 10 and 20 μM concentrations for 24 h. After incubation, the cells were washed with $1\times$ PBS twice to remove the residual drug and exposed to 1 mM of H_2O_2 and 500 μM of SIN-1 for 2 h and 4 h, respectively. These time periods were chosen on the basis of the observed cell death (>50%) using the H_2O_2 and SIN-1 concentrations mentioned above. Finally, cell viability was evaluated by the MTT reduction assay and calculated using eq 2.

Statistical Analysis. The experimental results are expressed as the mean \pm standard error of the mean (SEM) and are accompanied by the number (n) of observations. The differences between the groups were analyzed by student's *t* test. A *p* value lower than 0.05 was considered statistically significant.

Theoretical Evaluation of ADME Properties. The theoretical properties of log *P*, TPSA, *n*–OH, and *n*–OHNH were calculated by the methodology developed by Molinspiration using their software available on <http://www.molinspiration.com/services/properties.html>.

AUTHOR INFORMATION

Corresponding Author

*Phone: +34 981 563100. Fax: +34 981 544912. E-mail: svre77@gmail.com (S.V.-R.); colea@uchile.cl (C.O.-A.).

Notes

The authors declare no competing financial interest.

ACKNOWLEDGMENTS

This project was partially supported by CONICYT-Chile project 24110059, Mecsup project UCH-0601, and personal funds of Spanish researchers. F.P.C. thanks CONICYT-Chile for her Ph.D. grant and Fulbright Fellowships for her doctoral stay. S.V.R. thanks the Ministerio de Educación y Ciencia for her FPU Ph.D. grant, AP2008-04263 (Spain). M.J.M. thanks

Fundação para a Ciência e Tecnologia for her Ph.D. grant, SFRH/BD/61262/2009 (Portugal).

■ ABBREVIATIONS

AAPH, 2,2'-azobis(2-methylpropionamide)dihydrochloride; BAEC, bovine aortic endothelial cells; DCM, dichloromethane; DMEM, Dulbecco's modified Eagle's medium; DMPO, 5,5-dimethyl-1-pyrroline-*N*-oxide; DPPH, 2,2-diphenyl-1-picrylhydrazyl; Epa, anodic peak potential; FL, fluorescein; MAO, monoamine oxidase; MTT, 3-(4,5-dimethylthiazol-2-yl)-2,5-diphenyl-2*H*-tetrazolium bromide; ORAC, oxygen radical absorbance capacity; PBN, α -phenyl-*N*-*tert*-butylnitron; RNS, reactive nitrogen species; SIN-1, 3-morpholinopyridone; TBAP, tetrabutylammonium perchlorate; TLC, thin layer chromatography; TPSA, topological polar surface area; trolox, 6-hydroxy-2,5,7,8-tetramethylchroman-2-carboxylic acid

■ REFERENCES

- (1) Forman, H.; Maiorino, M.; Ursini, F. Signaling functions of reactive oxygen species. *Biochemistry*. **2010**, *49*, 835–842.
- (2) Lü, J. M.; Lin, P. H.; Yao, Q.; Chen, C. Chemical and molecular mechanisms of antioxidants: experimental approaches and model systems. *J. Cell. Mol. Med.* **2010**, *14*, 840–860.
- (3) Halliwell, B. Antioxidants and human diseases: a general introduction. *Nutr. Rev.* **1997**, *55*, 44–52.
- (4) Korkina, L. G.; Afans'Ev, I. B. Antioxidant and chelating properties of flavonoids. *Adv. Pharmacol.* **1996**, *38*, 151–163.
- (5) Yin, H.; Xu, L.; Porter, N. A. Free radical lipid peroxidation: mechanisms and analysis. *Chem. Rev.* **2011**, *111*, 5944–5972.
- (6) Sies, H. Oxidative stress: oxidants and antioxidants. *Exp. Physiol.* **1997**, *82*, 291–295.
- (7) Traykova, M.; Kostova, I. Coumarin derivatives and oxidative stress. *Int. J. Pharm.* **2005**, *1*, 29–32.
- (8) Obrenovich, M. E.; Li, Y.; Parvathaneni, K.; Yendluri, B. B.; Palacios, H. H.; Leszek, J.; Aliev, G. Antioxidants in health, disease and aging. *CNS Neurol. Disord.: Drug Targets* **2011**, *10*, 192–207.
- (9) Zou, X. Q.; Peng, S. M.; Hu, C. P.; Tan, L. F.; Deng, H. W.; Li, Y. J. Furoxan nitric oxide donor coupled chrysin derivatives: synthesis and vasculoprotection. *Bioorg. Med. Chem. Lett.* **2011**, *21*, 1222–1226.
- (10) Liu, R. H.; Hotchkiss, J. H. Potential genotoxicity of chronically elevated nitric oxide: a review. *Mutat. Res.* **1995**, *339*, 73–89.
- (11) Geier, D. A.; Kern, J. K.; Garver, C. R.; Adams, J. B. Audhya, T.; Nataf, R.; Geier, M. R. Biomarkers of environmental toxicity and susceptibility in autism. *J. Neurol. Sci.* **2009**, *280*, 101–108.
- (12) Pasupathi, P.; Chandrasekar, V.; Kumar, U. S. Evaluation of oxidative stress, enzymatic and non-enzymatic antioxidants and metabolic thyroid hormone status in patients with diabetes mellitus. *Diabetes Metab. Syndr.: Clin. Res. Rev.* **2009**, *3*, 160–165.
- (13) Reuter, S.; Gupta, S. C.; Chaturvedi, M. M.; Aggarwal, B. B. Oxidative stress, inflammation, and cancer: how are they linked? *Free Radical Biol. Med.* **2010**, *49*, 1603–1616.
- (14) Lodovici, M.; Menichetti, S.; Vighianisi, C.; Giuliani, E. Polyhydroxylated 4-thiaflavans as multipotent antioxidants: Protective effect on oxidative DNA damage in vitro. *Bioorg. Med. Chem. Lett.* **2006**, *16*, 1957–1960.
- (15) Heim, K. E.; Tagliaferro, A. R.; Bobilya, D. J. Flavonoid antioxidants: chemistry, metabolism and structure-activity relationships. *J. Nutr. Biochem.* **2002**, *13*, 572–584.
- (16) Khlebnikov, A. I.; Schepetkin, I. A.; Domina, N. G.; Kirpotina, L. N.; Quinn, M. T. Improved quantitative structure-activity relationship models to predict antioxidant activity of flavonoids in chemical, enzymatic, and cellular systems. *Bioorg. Med. Chem.* **2007**, *15*, 1749–1770.
- (17) Kostova, I.; Bhatia, S.; Grigorov, P.; Balkansky, S.; Parmar, V. S.; Prasad, A. K.; Saso, L. Coumarin as antioxidants. *Curr. Med. Chem.* **2011**, *18*, 3929–3951.
- (18) Torres de Pinedo, A.; Peñalver, P.; Morales, J. C. Synthesis and evaluation of new phenolic-based antioxidants: structure–activity relationship. *Food Chem.* **2007**, *103*, 55–61.
- (19) Haenen, G. R. M. M.; Arts, M. J. T. J.; Bast, A.; Coleman, M. D. Structure and activity in assessing antioxidant activity in vitro and in vivo: A critical appraisal illustrated with the flavonoids. *Environ. Toxicol. Pharmacol.* **2006**, *21*, 191–198.
- (20) Perez-Cruz, F.; Serra, S.; Delogu, G.; Lapier, M.; Maya, J. D.; Olea-Azar, C.; Santana, L.; Uriarte, E. Antitrypanosomal and antioxidant properties of 4-hydroxycoumarins derivatives. *Bioorg. Med. Chem. Lett.* **2012**, *22*, 5569–5573.
- (21) Matos, M. J.; Perez-Cruz, F.; Vazquez-Rodriguez, S.; Uriarte, E.; Santana, L.; Borges, F.; Olea-Azar, C. Remarkable antioxidant properties of a series of hydroxy-3-arylcoumarins. *Bioorg. Med. Chem.* **2013**, *21*, 3900–3906.
- (22) Kondo, K.; Hirano, R.; Matsumoto, A.; Igarashi, O.; Itakura, H. Inhibition of LDL oxidation by cocoa. *Lancet.* **1996**, *348*, 1514–1518.
- (23) Mazur, A.; Bayle, D.; Lab, C.; Rock, E.; Rayssiguier, Y. Inhibitory effect of procyanidin-rich extracts on LDL oxidation in vitro. *Atherosclerosis* **1999**, *145*, 421–422.
- (24) Ferrali, M.; Signorini, C.; Caciotti, B.; Sugherini, L.; Ciccoli, L.; Giachetti, D.; Comporti, M. Protection against oxidative damage of erythrocyte membranes by the flavonoid quercetin and its relation to iron chelating activity. *FEBS Lett.* **1997**, *416*, 123–129.
- (25) Elliott, A. J.; Scheiber, S. A.; Thomas, C.; Pardini, R. S. Inhibition of glutathione reductase by flavonoids. *Biochem. Pharmacol.* **1992**, *44*, 1603–1608.
- (26) Hirano, R.; Sasamoto, W.; Matsumoto, A.; Itakura, H.; Igarashi, O.; Kondo, K. Antioxidant ability of various flavonoids against DPPH radicals and LDL oxidation. *J. Nutr. Sci. Vitaminol.* **2001**, *47*, 357–362.
- (27) Cos, P.; Ying, L.; Calomme, M.; Hu, J. P.; Cimanga, K.; Van Poel, B.; Pieters, L.; Vlietnck, A. J.; Vanden Berghe, D. Structure-activity relationship and classification of flavonoids as inhibitors of xanthine oxidase and superoxide scavengers. *J. Nat. Prod.* **1998**, *61*, 71–76.
- (28) Sahu, N. K.; Balbhadra, S. S.; Choudhary, J.; Kohli, D. V. Exploring pharmacological significance of chalcone scaffold: a review. *Curr. Med. Chem.* **2012**, *19*, 209–225.
- (29) Go, M. L.; Wu, X.; Liu, X. L. Chalcones: an update on cytotoxic and chemoprotective properties. *Curr. Med. Chem.* **2005**, *12*, 483–499.
- (30) Bandgar, B. P.; Gawande, S. S.; Bodade, R. G.; Gawande, N. M.; Khobragade, C. N. Synthesis and biological evaluation of a novel series of pyrazole chalcones as anti-inflammatory, antioxidant and antimicrobial agents. *Bioorg. Med. Chem.* **2009**, *17*, 8168–8173.
- (31) Gaikwad, P.; Priyadarsini, K. I.; Naumov, S.; Rao, B. S. M. Radiation and quantum chemical studies of chalcone derivatives. *J. Phys. Chem. A.* **2010**, *114*, 7877–7885.
- (32) Detsi, A.; Majdalani, M.; Kontogiorgis, C. A.; Hadjipavlou-Litina, D.; Kefalas, P. Natural and synthetic 2'-hydroxy-chalcones and aurones: synthesis, characterization and evaluation of the antioxidant and soybean lipoxygenase inhibitory activity. *Bioorg. Med. Chem.* **2009**, *17*, 8073–8085.
- (33) Kumar, V.; Kumar, S.; Hassan, M.; Wu, H.; Thimmulappa, R. K.; Kumar, A.; Sharma, S. K.; Parmar, V. S.; Biswal, S.; Malhotra, S. V. Novel chalcone derivatives as potent Nrf2 activators in mice and human lung epithelial cells. *J. Med. Chem.* **2011**, *54*, 4147–4159.
- (34) Valdameri, G.; Gauthier, C.; Terreux, R.; Kachadourian, R.; Day, B. J.; Winnischofer, S. M. B.; Rocha, M. E. M.; Frchet, V.; Ronot, X.; Di Pietro, A.; Boumendjel, A. Investigation of chalcones as selective inhibitors of the breast cancer resistance protein: critical role of methoxylation in both inhibition potency and cytotoxicity. *J. Med. Chem.* **2012**, *55*, 3193–3200.
- (35) Kachadourian, R.; Day, B. J.; Pugazhenti, S.; Franklin, C. C.; Genoux-Bastide, E.; Mahaffey, G.; Gauthier, C.; Di Pietro, A.; Boumendjel, A. A synthetic chalcone as a potent inducer of glutathione biosynthesis. *J. Med. Chem.* **2012**, *55*, 1382–1388.
- (36) Jung, J. C.; Jang, S.; Lee, Y.; Min, D.; Lim, E.; Jung, H.; Oh, M.; Oh, S.; Jung, M. Efficient synthesis and neuroprotective effect of

substituted 1,3-diphenyl-2-propen-1-ones. *J. Med. Chem.* **2008**, *51*, 4054–4058.

(37) (a) Borges, F.; Roleira, F.; Milhazes, N.; Santana, L.; Uriarte, E. Simple coumarins and analogues in medicinal chemistry: occurrence, synthesis and biological activity. *Curr. Med. Chem.* **2005**, *12*, 887–916.

(b) Rao, H. S. P.; Tangeti, V. S. Synthesis of 3-aryl coumarin-flavone hybrids. *Lett. Org. Chem.* **2012**, *9*, 218–220. (c) Rao, H. S. P.; Sivakumar, S. Condensation of α -aroyl ketene dithioacetals and 2-hydroxyarylaldehydes results in facile synthesis of a combinatorial library of 3-aryl coumarins. *J. Org. Chem.* **2006**, *71*, 8715–8723.

(38) Matos, M. J.; Vazquez-Rodriguez, S.; Santana, L.; Uriarte, E.; Fuentes-Edrúf, C.; Santos, Y.; Muñoz-Crego, A. Looking for new targets: simple coumarins as antibacterial agents. *Med. Chem.* **2012**, *8*, 1140–1145.

(39) Matos, M. J.; Ferino, G.; Cadoni, E.; Laguna, R.; Borges, F.; Uriarte, E.; Santana, L. 8-Substituted 3-aryl coumarins as potent and selective MAO-B inhibitors: synthesis, pharmacological evaluation, and docking studies. *ChemMedChem* **2012**, *7*, 464–470.

(40) Matos, M. J.; Vazquez-Rodriguez, S.; Uriarte, E.; Santana, L.; Viña, D. MAO inhibitory activity modulation: 3-phenyl coumarins versus 3-benzoyl coumarins. *Bioorg. Med. Chem. Lett.* **2011**, *21*, 4224–4227.

(41) Secci, D.; Carradori, S.; Bolasco, A.; Chimenti, P.; Yañez, M.; Ortuso, F.; Alcaro, S. Synthesis and selective human monoamine oxidase inhibition of 3-carbonyl, 3-acyl, and 3-carboxyhydrazido coumarin derivatives. *Eur. J. Med. Chem.* **2011**, *46*, 4846–4852.

(42) Serra, S.; Chicca, A.; Delogu, G.; Vazquez-Rodriguez, S.; Santana, L.; Uriarte, E.; Casu, L.; Gertsch, J. Synthesis and cytotoxic activity of non-naturally substituted 4-oxycoumarin derivatives. *Bioorg. Med. Chem. Lett.* **2012**, *22*, 5791–5794.

(43) Vazquez-Rodriguez, S.; Matos, M. J.; Santana, L.; Uriarte, E.; Borges, F.; Kachler, S.; Klotz, K. N. Chalcone-based derivatives as new scaffolds for hA₃ adenosine receptor antagonists. *J. Pharm. Pharmacol.* **2013**, *65*, 697–703.

(44) Brunet, E.; Alonso, M. T.; Juanes, O.; Velasco, O.; Rodríguez-Ubis, J. C. Novel polyaminocarboxylate chelates derived from 3-aryl coumarins. *Tetrahedron* **2001**, *57*, 3105–3116.

(45) Janzen, E. G.; Kotake, Y.; Randall, D. H. Stabilities of hydroxyl radical spin adducts of PBN-type spin traps. *Free Radical Biol. Med.* **1992**, *12*, 169–173.

(46) Ou, B.; Hampsch-Woodill, M.; Prior, R. L. Development and validation of an improved oxygen radical absorbance capacity assay using fluorescein as the fluorescent probe. *J. Agric. Food Chem.* **2001**, *49*, 4619–4626.

(47) Clothier, R.; Gómez-Lechón, M. J.; Kinsner-Ovaskainen, A.; Kopp-Schneider, A.; O'Connor, J. E.; Prieto, P.; Stanzel, S. Comparative analysis of eight cytotoxicity assays evaluated within the ACuteTox Project. *Toxicol. In Vitro* **2012**, *27*, 1347–1356.

(48) Singgh, R. J.; Hogg, N.; Joseph, J.; Konorev, E.; Kalyanaraman, B. The peroxy nitrite generator, SIN-1, becomes a nitric oxide donor in the presence of electron acceptors. *Arch. Biochem. Biophys.* **1999**, *361*, 331–339.

(49) *M cheminformatics*. <http://www.molinspiration.com/services/properties.html>, Bratislava, Slovak Republic.

(50) Vogel, S.; Barbic, M.; Jürgenliemk, G.; Heilmann, J. Synthesis, cytotoxicity, anti-oxidative and anti-inflammatory activity of chalcones and influence of A-ring modifications on the pharmacological effect. *Eur. J. Med. Chem.* **2010**, *45*, 2206–2213.

(51) Zhang, H. Y.; Wang, L. F. Theoretical elucidation of structure-activity relationship for coumarins to scavenge peroxy radical. *J. Mol. Struct.: THEOCHEM* **2004**, *673*, 199–202.

(52) Saprín, A. N.; Piette, L. H. Spin trapping and its application in the study of lipid peroxidation and free radical production with liver microsomes. *Arch. Biochem. Biophys.* **1977**, *180*, 480–492.

(53) Durand, G.; Proszak, R. A.; Han, Y.; Ortial, S.; Rockenbauer, A.; Pucci, B.; Villamena, F. A. Spin trapping and cytoprotective properties of fluorinated amphiphilic carrier conjugates of cyclic versus linear nitrones. *Chem. Res. Toxicol.* **2009**, *22*, 1570–1581.

(54) Galati, G.; Moridani, M. Y.; Chan, T. S.; O'Brien, P. J. Peroxidative metabolism of apigenin and naringenin versus luteolin and quercetin: glutathione oxidation and conjugation. *Free Radical Biol. Med.* **2001**, *30*, 370–382.

(55) Bast, A.; Haenen, G. R. M. M. The toxicity of antioxidants and their metabolites. *Environ. Toxicol. Pharmacol.* **2002**, *11*, 251–258.

(56) Lipinski, C. A.; Lombardo, F.; Dominy, B. W.; Feeney, P. J. Experimental and computational approaches to estimate solubility and permeability in drug discovery and development settings. *Adv. Drug Delivery Rev.* **1997**, *23*, 3–25.

(57) Ertl, P.; Rohde, B.; Selzer, P. Fast calculation of molecular polar surface area as a sum of fragment-based contributions and its application to the prediction of drug transport properties. *J. Med. Chem.* **2000**, *43*, 3714–3717.

(58) Buu-Hoi, N. P.; Loc, T. B.; Xuong, N. D. 3-(*p*-Hydroxyaroyl)- and -(*p*-methoxyaroyl)coumarins. *Bull. Soc. Chim. Fr.* **1958**, *3*, 361–363.

(59) Huang, D.; Ou, B.; Hampsch-Woodill, M.; Flanagan, J. A.; Prior, R. L. High-throughput assay of oxygen radical absorbance capacity (ORAC) using a multichannel liquid handling system coupled with a microplate fluorescence reader in 96-well format. *J. Agric. Food Chem.* **2002**, *50*, 4437–4444.

(60) Parker, T. L.; Miller, S. A.; Myers, L. E.; Miguez, F. E.; Engeseth, N. J. Evaluation of synergistic antioxidant potential of complex mixtures using oxygen radical absorbance capacity (ORAC) and electron paramagnetic resonance (EPR). *J. Agric. Food Chem.* **2010**, *58*, 209–217.

(61) Yoshimura, Y.; Inomata, T.; Nakazawa, H.; Kubo, H.; Yamaguchi, F.; Ariga, T. Evaluation of free radical scavenging activities of antioxidants with an H₂O₂/NaOH/DMSO system by electron spin resonance. *J. Agric. Food Chem.* **1999**, *47*, 4653–4656.

(62) Das, A.; Chakrabarty, S.; Choudhury, D.; Chakrabarti, G. 1,4-Benzoquinone (PBQ) induced toxicity in lung epithelial cells is mediated by the disruption of the microtubule network and activation of caspase-3. *Chem. Res. Toxicol.* **2010**, *23*, 1054–1066.

(63) Das, A.; Bhattacharya, A.; Chakrabarti, G. Cigarette smoke extract induces disruption of structure and function of tubulin-microtubule in lung epithelium cells and in vitro. *Chem. Res. Toxicol.* **2009**, *22*, 446–459.